Journal of Solid State Chemistry **155,** 372–380 (2000)
doi:10.1006/jssc.2000.8927, available online at http://www.idealibrary.com on IDEAL®

Phase Transition Induced by High Pressure in a New $LaBaCuGaO_5$ Compound

M. L. Ruiz-González, J. Ramírez-Castellanos, and J. M. González-Calbet[1]

Dpto. Química Inorgánica, Facultad de Químicas, Universidad Complutense, 28040 Madrid, Spain

Received March 31, 2000; in revised form August 8, 2000; accepted August 9, 2000; published online November 29, 2000

The structure of a new $LaBaCuGaO_5$ material has been elucidated by means of X-ray diffraction (XRD), selected-area electron diffraction (SAED), and high-resolution transmission electron microscopy (HRTEM). This oxide shows the brownmillerite-type structure, built-up of alternating octahedral and tetrahedral layers sharing corners with space group *Ima*2 and lattice parameters $a = 1.6707$ nm, $b = 0.5511$ nm, and $c = 0.5485$ nm. The presence of some structural disorder at the equatorial oxygen is discussed. When this material is treated under high pressure a phase transition takes place. Although X-ray diffraction data suggest an average cubic perovskite structure, electron diffraction and microscopy show the presence of perpendicular microdomains constituted by the intergrowth of some perovskite-related superstructures. Paramagnetic behavior is observed in all cases.

Key Words: **$LaBaCuGaO_5$; high pressure; microstructure; electron microscopy.**

INTRODUCTION

The flexibility of mixed oxides having ABO_3 perovskite-related structures to adopt different chemical substitutions without undergoing drastic structural changes is well known. This is possible because of the ability of several cations occupying *B* sites to adopt different environments and/or different oxidation states. In some cases, as in the case of copper mixed oxides, high pressure has been a very useful tool for stabilizing new phases, since it can induce phase transitions, for stabilizing nonhabitual oxidation states, for increasing coordination indexes, and for enhancing the solubility limits.

These two facts—perovskite flexibility and high-pressure synthesis—have had a great impact on the search for new high-temperature superconducting materials. For instance, Isobe *et al.* (1) and Takayama-Muromachi and Isobe (2) have reported a new homologous series of high-pressure-synthesized superconductors with the general formula $GaSr_2Ca_{n-1}Cu_nO_{2n+3}$. Their structures (3) can be described as formed by the alternation of n $[CuO_2]$ layers with one $[GaO_4]$ tetrahedral layer, occurring between $(n-1)$ Ca and SrO layers, along the *c* axis, according to the stacking sequence …–GaO–SrO–CuO_2–$[Ca–CuO_2]_{n-1}$–SrO–…

Sr_2CuGaO_5 would be the $n = 1$ term of this series if all copper were Cu(III). Following the features of the previous structures, the $n = 1$ member should be formed by octahedral $[CuO_6]$ layers alternating in an ordered way along the *c* axis with tetrahedral $[GaO_4]$ layers, leading to a brownmillerite-type structure (4), the periodicity of these layers being …OTOT'… due to a tilt between tetrahedral layers. Such an oxide term has not yet been isolated. However, the introduction of 50% of La in the *A* positions of the perovskite sublattice has led to the stabilization of the brownmillerite-type structure when $LaSrCuGaO_5$ (5–7) and $LaCaCuGaO_5$ (8) are synthesized at room pressure. No data have been reported for the analogous $LaBaCuGaO_5$.

In this paper, we describe the synthesis and the structural characterization of $LaBaCuGaO_5$ by means of selected-area electron diffraction (SAED) and high-resolution transmission electron microscopy (HRTEM). The effect of the high pressure on the structure is discussed.

EXPERIMENTAL

The room pressure (RP) sample with nominal composition $LaBaCuGaO_5$ was prepared from stoichiometric amounts of La_2O_3 (previously heated at 950°C in air to remove any trace of water or carbonate), CuO, Ga_2O_3, and $BaCO_3$. The mixture was ground and mixed in an agate mortar and heated, after carbonate decomposition, at 1000°C for 170 h with intermediate grindings.

This product was the starting material for the synthesis of the high-pressure (HP) sample, using a conventional cubic-anvil-type apparatus (9). The sample was allowed to react at 6 GPa and 1000°C for 30 min, and then was quenched at ambient temperature while pressure was slowly released.

[1]To whom correspondence should be addressed. Fax: 91 394 43 52. E-mail: jgcalbet@eucmax.sim.ucm.es.

0022-4596/00 $35.00

Powder X-ray diffraction (XRD) patterns were recorded using a Philips X'-Pert diffractometer with Cu$K\alpha$ radiation. Chemical compositions were determined by energy dispersive X-ray microanalysis spectroscopy (EDS) on a JEOL 2000 FX microscope equipped with a LINK System AN10000EXL. SAED and HRTEM were carried out on both JEOL 2000-FX and JEOL 4000-EX microscopes. Magnetic susceptibility measurements, in the range of 5 to 300 K and in a 100-Oe applied field, were performed in a SQUID MPMS-XL magnetometer.

RESULTS AND DISCUSSION

(a) RP Sample

All XRD maxima can be indexed on the basis of a brownmillerite structure with space group *Ima*2 and lattice parameters $a = 1.6707(2)$ nm, $b = 0.5511(2)$ nm, and $c = 0.5485(2)$ nm, except two small peaks due to the presence of $LaBaGa_3O_7$ as an impurity. This situation is similar to that described for $LaSrCuGaO_5$ (5–7), which always appears with an impurity corresponding to $LaSrGa_3O_7$.

The analysis by EDS also suggests the presence of two phases, in agreement with the XRD study. The major one shows the $La_{1.17}Ba_{0.95}Cu_{1.20}Ga_{0.73}O_5$ composition, where the Cu:Ga ratio clearly deviates from the ideal value 1:1, being a gallium-deficient phase. However, with the $La_{1.07}Ba_{1.08}Cu_{0.16}Ga_{2.77}O_7$ composition the impurity phase is a gallium-rich phase.

SAED and HRTEM data confirm the structural features characteristic of the brownmillerite-type structure. However, a more complex situation is observed. The SAED patterns along [010] and [01$\bar{1}$] zone axes (Figs. 1a and b, respectively) show (i) strong spots, in agreement with the *Ima*2 space group, and (ii) diffuse streaking along alternating rows parallel to the a^* direction (as marked by arrows in the figures), suggesting the existence of some disorder along the a axis. However, the corresponding micrographs (Figs. 2a and 3a) are characteristic of an ordered material with a brownmillerite structure. The periodicity along the a direction is seemingly $a/2 = 0.83$ nm, as expected from the basic structure. The rows of highest contrast should correspond to Ga layers, which are separated by 0.83 nm. A different contrast can be observed between Cu and Ga layers, as a result of the ordering between both cations, separated by La and Ba planes.

To confirm this model, a HRTEM image simulation using the MacTempas software (10) was performed, introducing the atomic coordinates characteristic of the *Ima*2 space group (8) and considering both an ordered and a random arrangement of the La and Ba cations. A good fit to the experimental images was found in the last case, i.e., when La and Ba were randomly distributed on their lattice positions, as can be observed in the simulated images in Fig. 2b

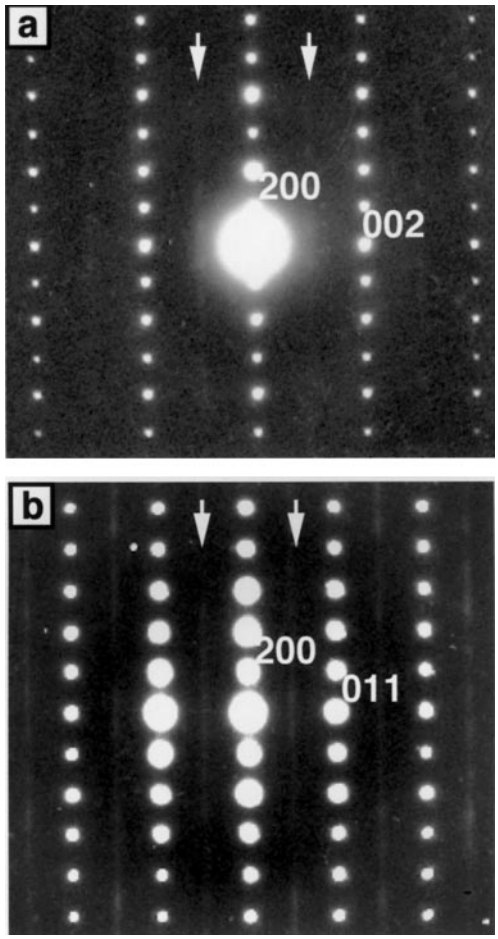

FIG. 1. SAED patterns along (a) [010] and (b) [01$\bar{1}$] directions corresponding to $LaBaCuGaO_5$ (RP).

corresponding to the [010] zone axis ($\Delta f = -55$ and $\Delta t = 1$ nm) (f = defocus and t = thickness) and Fig. 3b along the [01$\bar{1}$] zone axis ($\Delta f = -20$ and $\Delta t = 3$ nm). Through focus and thickness simulated images are shown in Fig. 4. According to that, the $LaBaCuGaO_5$ shows a brownmillerite structure where CuO_6 octahedra and GaO_4 tetrahedra layers, sharing corners, alternate along the a direction. A projection of the structure along [01$\bar{1}$] is depicted in Fig. 3c.

In a previous study (6) of a single crystal of the related material $LaSrCuGaO_5$, random distribution of the La and Sr atoms at A positions of the $A_2B_2O_5$ brownmillerite structure was established. However, Kharlanov *et al.* (7), from HRTEM images, proposed two structural models, considering both order (model I) or disorder (II) of La and Sr cations. These authors concluded that model I better explained the experimental images. However, the simulated images in both cases are quite similar, with unusually high thermal parameters.

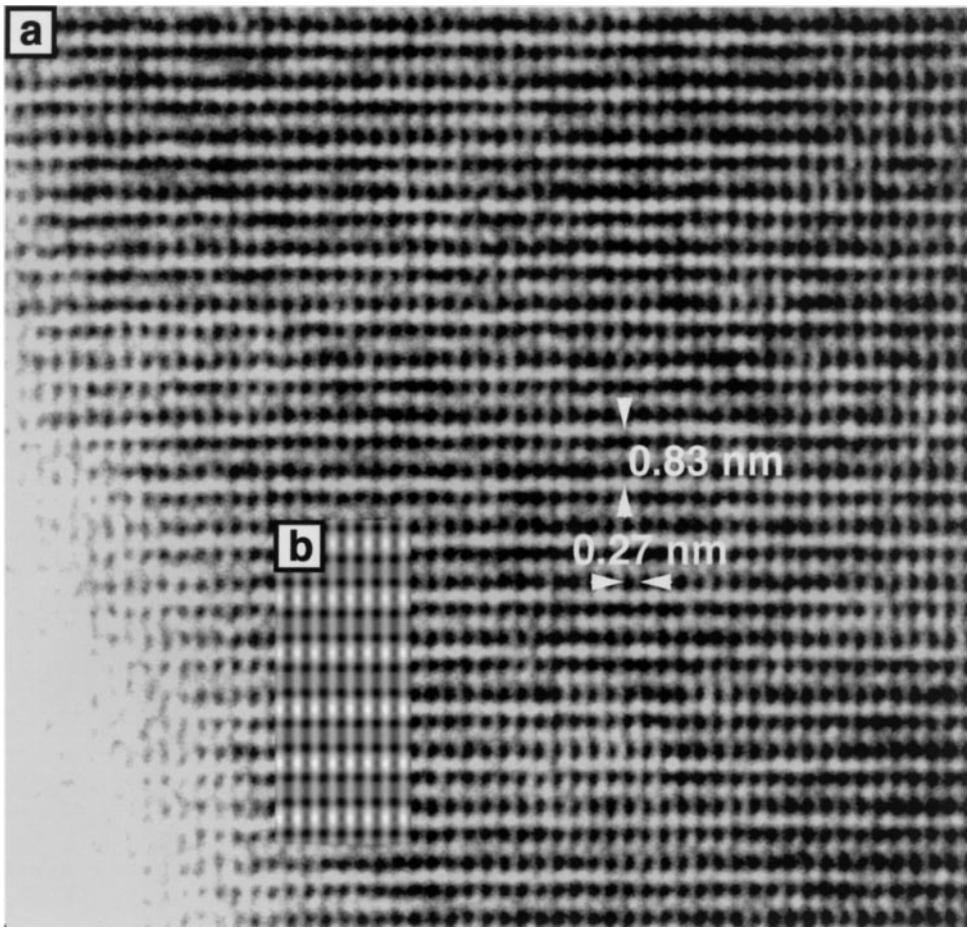

FIG. 2. (a) HRTEM micrograph along the [010] direction and (b) corresponding calculated image for $LaBaCuGaO_5$ (RP).

Nevertheless, the streaking in the SAED patterns has not yet been explained. A disordered distribution of Ga and Cu sites should be reflected in the HRTEM image, since contrast is mainly due to the cation contribution. Therefore, it can be assumed that streaking could be due to some disorder in the oxygen positions, mainly in the equatorial oxygens of the GaO_4 tetrahedra, which are the more labile positions of the brownmillerite structural type. It is worth emphasizing, however, that according to EDS data the sample has some copper excess compared with gallium; therefore, some Cu must be randomly distributed in square planar coordination, replacing Ga in tetrahedral coordination. These two effects could give rise to local changes at the oxygen positions in the *Ima*2 space group. In this case, it is worth mentioning that the agreement between experimental and calculated images along the [010] zone axis is not complete, since white contrasts corresponding to the calculated image show a slight elongation with respect to the experimental one. Such a difference can be understood, as previously discussed, by taking into account that the proposed model is an idealized one that places the oxygen atoms over the atomic positions corresponding to the *Ima*2 space group. In fact, two space groups are possible for this structure. It is known that the own mineral $Ca_2(Fe,Al)_2O_5$ (11) crystallizes in an *Ima*2 space group, but the isostructural $Ca_2Fe_2O_5$ (4) shows the *Pnma* space group. The difference between the two is just the arrangement of the oxygens in the $x = 3/4$ tetrahedral layer. These data suggest that the structure consists of main blocks, showing the *Ima*2 brownmillerite structure, and clusters randomly dispersed where the equatorial oxygens occupy the position characteristic of the space group *Pnma*.

Some examples have been reported showing the structural changes produced by the oxygen movement. $Sr_2Co_2O_5$ (12) undergoes, under the electron beam, a reversible phase transition. It seems obvious that the beam intensity plays an important role, but it is difficult to say if the transition is due either to the local temperature of the crystal or to the impulse transference of the electrons. This structural change has been attributed to a rearrangement of the oxygen sublattice, since the oxygen atoms are the lightest.

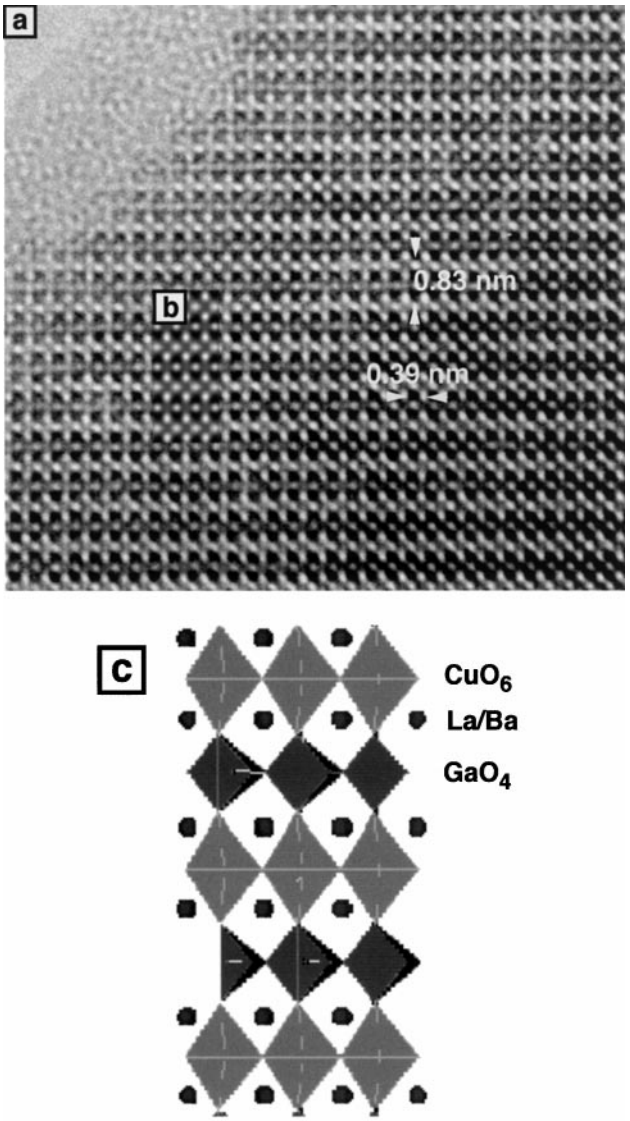

FIG. 3. (a) HRTEM micrograph along the [01$\bar{1}$] direction, (b) corresponding calculated image for $LaBaCuGaO_5$ (RP), and (c) idealized structural model showing the atomic positions.

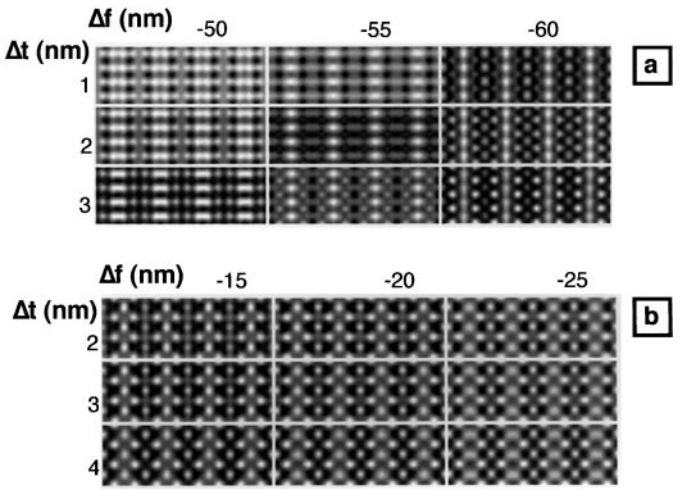

FIG. 4. Simulated brownmillerite images as a function of thickness and defocus along (a) [01$\bar{1}$] and (b) [010] zone axes, respectively.

In the case of $LaBaCuGaO_5$, it seems that a slight movement of the oxygens at equatorial positions, either in the GaO_4 tetrahedra or in the CuO_4 square planes, can be produced in order to reduce lattice tensions created by Ba^{2+} due to its considerable size. This situation would keep the layer sequence characteristic of the brownmillerite, while justifying the streaking observed in the SAED patterns. In this sense, it seems interesting to compare such disorder with that observed in $n = 3$ and 4 terms of the homologous series $GaSr_2Ca_{n-1}Cu_nO_{2n+3}$ (3) which, in this case, is due to an interlayer disorder, along a, of two types of GaO_4 tetrahedral chains alternating in an ordered way along the b axis.

Diffuse streaking only appears along certain directions such as [0$\bar{2}$1] and [0$\bar{3}$2] and the corresponding HREM image reflects the expected disorder.

Magnetic data showed paramagnetic behavior (Fig. 5). The calculated magnetic moment following the Curie–Weiss law is 1.73 μ_B, in good agreement with the theoretical one if only Cu(II) is considered to exist in the material. This behavior seems to be consistent with the commonly accepted idea that the mixed valence of copper is necessary for the existence of superconductivity, inducing p-type superconductivity only if Cu(II) and (III) coexist. In this way, it is worth mentioning that the material shows a brownmillerite structure, suggesting that all oxygen positions in the Cu–O blocks are occupied; therefore, there are no oxygen-deficient layers giving rise to extended two-dimensional $Cu–O_2$ planes, which appears to be necessary for the existence of superconductivity.

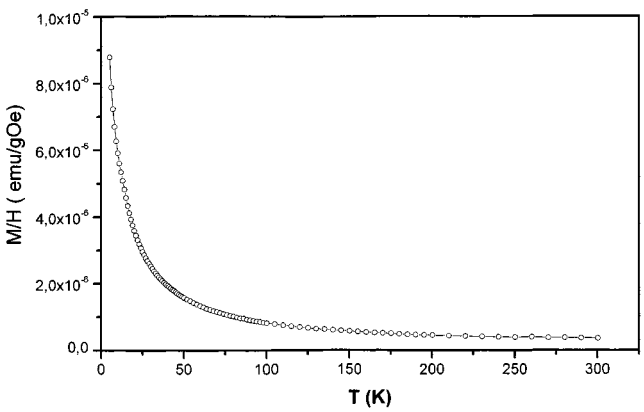

FIG. 5. Magnetic susceptibility vs temperature for $LaBaCuGaO_5$ (RP).

(b) HP Sample

The XRD pattern can be indexed on the basis of a cubic perovskite structure with $a_c = 0.393$ nm, indicating that a structural phase transition has been induced by the application of high pressure to the RP material. The average composition obtained by microanalysis performed on several crystals is $La_{0.93}Ba_{0.89}Cu_{1.01}Ga_{0.85}O_y$, close to the nominal one. Slight differences can be understood taking into account that compositional homogeneity is not always found in high-pressure samples due to short reaction periods. Additional phases were not detected by both X-ray and electron diffraction.

Magnetic measurements indicate paramagnetic behavior. The calculated magnetic moment is 2.7 μ_B, in good agreement with the presence of some Cu^{3+} in the material, due to the partial oxidation of Cu(II) to Cu(III).

The SAED and HRTEM studies reveal again a more complicated situation, suggesting the existence of a perovskite-related superstructure. The SAED patterns along the $[100]_c$ and $[10\bar{1}]_c$ zone axes (Figs. 6a and 6b) show two sets of spots: (i) strong spots, which can be indexed on the basis of a cubic perovskite subcell, and (ii) diffuse spots at 2/5 and 3/5 of the main reflections. Subindex c refers to the perovskite cubic unit subcell.

The corresponding image along $[100]_c$ (Fig. 7a) shows two perpendicular domains as suggested in the SAED pattern. The contrast analysis in an enlarged micrograph (Fig. 7b) shows a disordered intergrowth between two areas with different d spacings (0.83 and 1.14 nm, respectively) that can be attributed to the following stacking sequences: (i) … OT …, characteristic of the brownmillerite structural type, and (ii) … OOT …, characteristic of the $A_3B_3O_8$ structure (13). Even more, a detailed study reveals a local ordered intergrowth, which would lead to either a 5- or a 10-fold superstructure of the basic perovskite, depending on the relative orientation of the tetrahedra in different layers, in agreement with the spots observed at 2/5 and 3/5 in the SAED patterns (Figs. 6a and 6b).

The changes observed under high pressure can be understood if we consider that Ga cations adopt octahedral coordination better than tetrahedral, giving rise to an … OOT … sequence. The large size of barium atoms in some extensions can avoid the overall … OT … → … OOT … transition, since the hole between two adjacent octahedral layers is not big enough to accommodate this cation.

To stabilize the … OOT … sequence and confirm the above proposal, the substitution of a smaller cation instead of Ba was carried out by preparing the $LaBa_xSr_{1-x}CuGaO_y$ system in the composition range $0.5 < x < 0.9$. From the XRD data, a decrease in the lattice parameters is observed as the Sr amount increases, due to the smaller ionic radius of this cation (14). Figure 8a shows the SAED pattern along

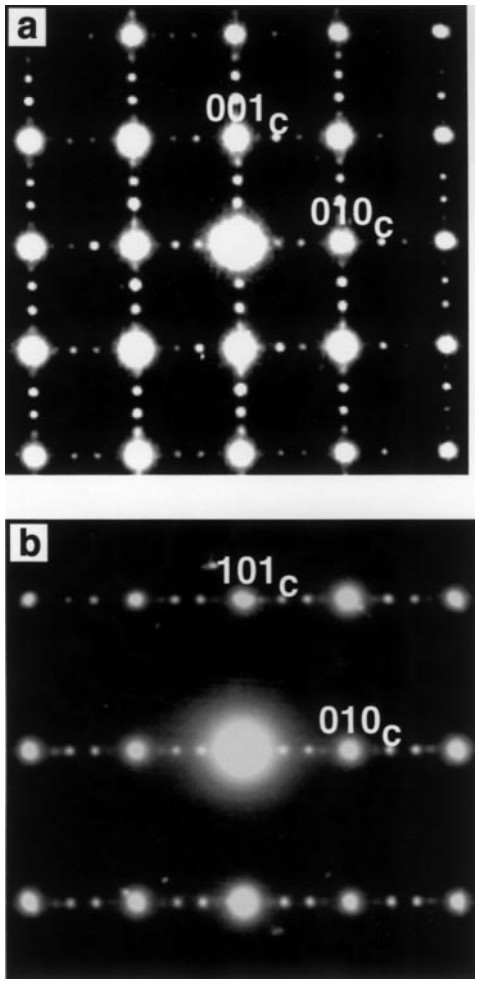

FIG. 6. SAED patterns along (a) $[100]_c$ and (b) $[10\bar{1}]_c$ directions corresponding to $LaBaCuGaO_5$ (HP).

$[100]_c$ for the $x = 0.5$ material. It can be observed that between the main reflections, which can be indexed using a cubic symmetry, two weaker ones exist along both b^* and c^* directions, suggesting the presence of perpendicular domains with a threefold superstructure of the cubic perovskite. In the corresponding HRTEM (Fig. 8b) the existence of microdomains is confirmed, where the interplanar distance between fringes is 1.14 nm, in good agreement with the stacking sequence … OOT …, as can be better seen in Fig. 8c. Similar results are found for higher x values; however, when x is close to 1, disordered intergrowths of the two stacking sequences, i.e., … OT … (0.83 nm) and … OOT … (1.14 nm), begin to appear, in agreement with the bigger size of the Ba cation, as can be seen in Fig. 9 corresponding to $LaBa_{0.9}Sr_{0.1}CuGaO_y$.

These structural features were also previously observed in the $Ca_2LaFe_3O_{8+\delta}$ material (15). For $\delta = 0$, this material shows the $A_3B_3O_8$ structure, i.e., a threefold superstructure

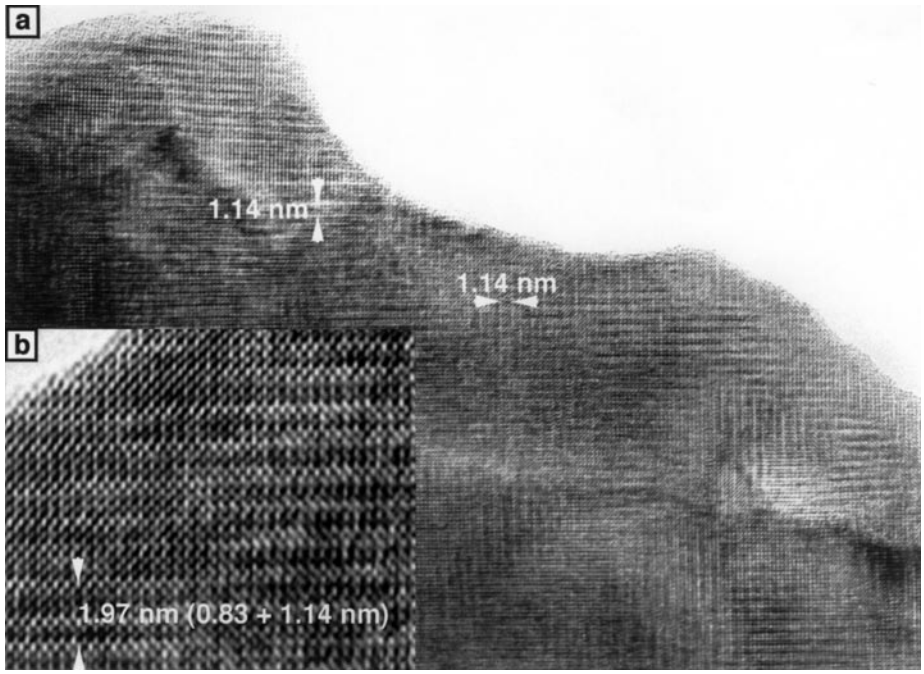

FIG. 7. (a) HRTEM micrograph along $[100]_c$ and (b) enlargement of one domain showing the disordered intergrowth.

of the cubic perovskite along the *b* direction, having an ordered sequence …OOT… On the other hand, for $\delta = 0.24$ the HRTEM study shows that three-dimensional microdomains intergrow within one crystal. Each of these domains have the $A_3B_3O_8$ structure, but the superstructure is randomly found along each of the three cubic subcell directions. Therefore, it seems that the oxidation process is accompanied by microdomain formation.

In our case, it seems clear that high pressure produces partial oxidation of $[GaO_4]_t$ to $[GaO_6]_o$ in $LaBaCuGaO_5$, leading to a change in the stacking sequence from …OT… to …OOT…, along the *b* direction of the structure, with microdomain formation. The Ga tendency to adopt octahedral coordination can stabilize the $LaBa_xSr_{1-x}CuGaO_5$ $(0 < x < 1)$ system with the $A_3B_3O_8$ structure.

It is worth emphasizing that such an …OOT… polyhedra sequence, due to the Ga tendency to adopt octahedral coordination, would keep the ordered cation arrangement …Ga–Cu–Ga–Cu…, only if Cu adopts tetrahedral coordination. However, this does not seem to be evident taking into account the usual coordination environment adopted by Cu cations: octahedral, square planar pyramidal, and square planar. In this sense, in order to have the …OOT… sequence, keeping the Ga:Cu relation equal to 1:1, with Ga and Cu in octahedral positions and only Ga in the tetrahedral ones, two kinds of cation arrangements, along *b*, could alternate: (i) $Ga_tCu_oGa_oGa_t$ and (ii) $Ga_tCu_oCu_oGa_t$ (t = tetrahedral coordination, o = octahedral coordination). If those sequences were stacked in an ordered way, a sixfold superstructure would be obtained, …$Ga_tCu_oGa_oGa_tCu_oCu_oGa_t$…, while a random distribution would lead to an average threefold superstructure.

From the experimental image, it is not easy to distinguish between ordered and disordered models, because the contrast transfer function of Ga_o and Cu_o must be close, but both are in agreement with the suggested …OOT… sequence as well as with the cation composition. Two image calculations were performed taking into account the $A_3B_3O_8$ structure (16) (space group, $Pmc2_1$). One of them, with Ga in tetrahedral positions, had octahedral positions occupied by Ga and Cu at 50%, i.e., following the sequence $Ga_tCu_oGa_oGa_t$. The other calculation involved Ga in tetrahedral positions and only Cu in octahedral position, i.e., the sequence $Ga_tCu_oCu_oGa_t$. In both models Ba was placed at the *A* positions closer to Ga_t while a disordered distribution of La/Sr was considered. Such a structural model ($A_3B_3O_8$) is depicted in Fig. 10d. The results of both calculations were identical; simulated images are shown in Fig. 11. A good fit was found between experimental and calculated images as can be observed in Fig. 10 corresponding to the $x = 0.6$ material along the $[100]_c$ zone axis ($\Delta f = -25$ nm and $\Delta t = 5$ nm). These facts seem to confirm (i) the …OOT… polyhedra sequence as well as (ii) the impossibility of distinguishing, by this technique, between an ordered and a disordered arrangement of the two sequences $Ga_tCu_oGa_oGa_t$ and $Ga_tCu_oCu_oGa_t$.

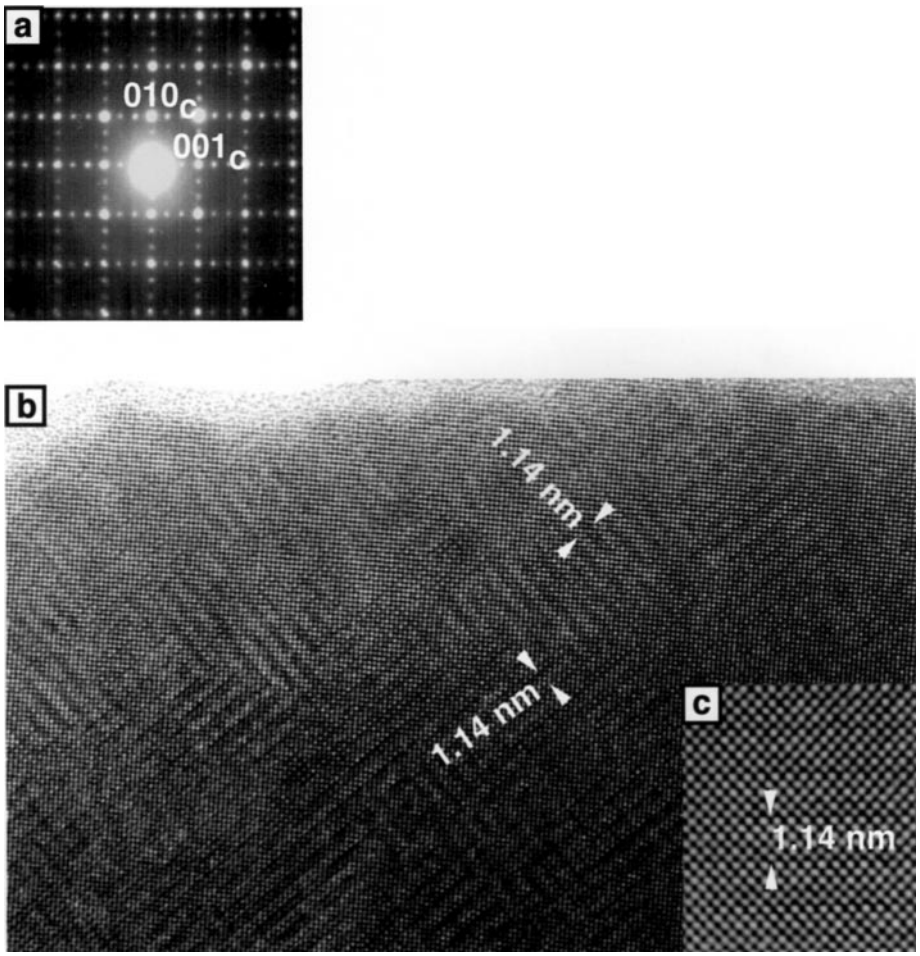

FIG. 8. (a) SAED pattern along the $[100]_c$ direction, (b) corresponding HRTEM micrograph for the HP material $LaBa_{0.5}Sr_{0.5}CuGaO_y$, and (c) enlargement of one domain showing the threefold superstructure characteristic of a sequence … OOT …

On the other hand, the same discussion can be extended for the $LaBaCuGaO_5$, where a fivefold order has been proposed, as a consequence of an ordered distribution of two sequences: (i) … OT … and (ii) … OOT … Again, two structural facts must be considered: (i) the ordered arrangement of Cu and Ga in alternating layers along *b* must be

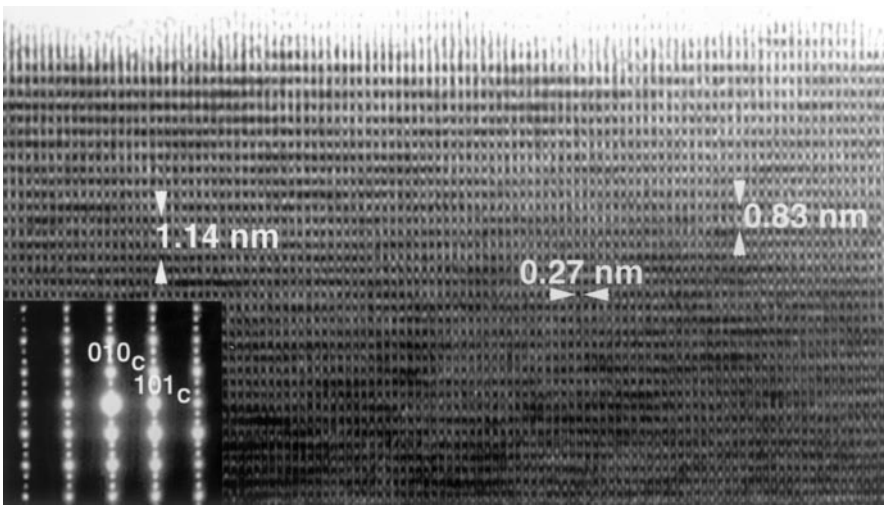

FIG. 9. SAED pattern along the $[10\bar{1}]_c$ direction and corresponding HRTEM micrograph for $LaBa_{0.9}Sr_{0.1}CuGaO_y$ (HP).

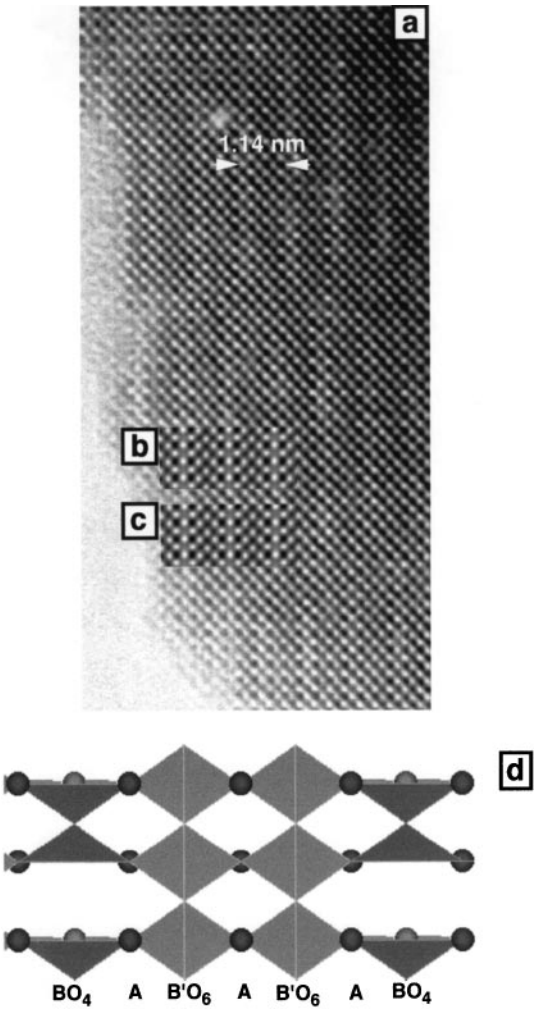

FIG. 10. (a) HRTEM micrograph along $[100]_c$, (b) image calculation for $LaBa_{0.6}Sr_{0.4}CuGaO_y$ (HP) considering the $Ga_tCu_oGa_oGa_t$ sequence, (c) considering the $Ga_tCu_oCu_oGa_t$ sequence, and (d) structural model showing the $\ldots OOT \ldots$ stacking sequence, being $B = Ga$ and $B' = Ga, Cu$.

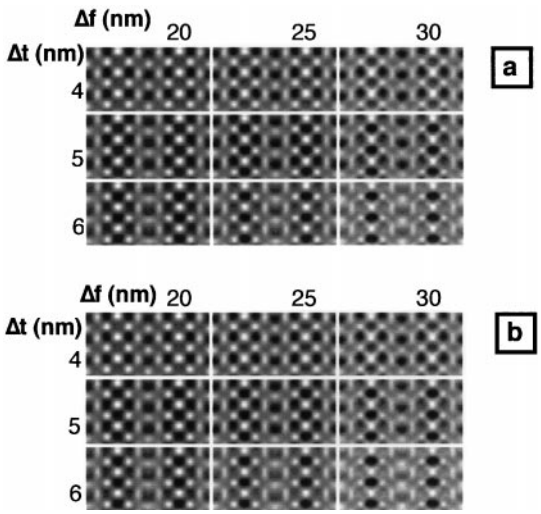

FIG. 11. Simulated $A_3B_3O_8$ images as a function of thickness and defocus along the $[100]_c$ zone axis considering (a) the $Ga_tCu_oGa_oGa_t$ sequence and (b) the $Ga_tCu_oCu_oGa_t$ sequence.

broken in the $\ldots OOT \ldots$ sequence; (ii) there must be two $\ldots OOT \ldots$ sequences with different compositions, $Ga_tCu_oGa_oGa_t$ and $Ga_tCu_oCu_oGa_t$, because only in this way can the Ga:Cu relation be kept equal to 1. The $\ldots OT \ldots$ sequence must be the one observed in the ambient pressure material, i.e., $\ldots Ga_tCu_o \ldots$ characteristic of a brownmillerite structure.

Finally, it is worth mentioning that susceptibility measurements indicate paramagnetic behavior and suggest the presence of Cu^{3+} in the high-pressure $LaBa_xSr_{1-x}CuGaO_y$ samples, in good agreement with the proposed structural models, which involve an increase in oxygen content. On the other hand, it is well known that two-dimensional CuO_2 sheets, as well as a mixture of both Cu^{2+} and Cu^{3+}, are thought to be necessary to obtain superconductivity. In this sense, both oxidation states seem to be present in the high-pressure samples; however, as in the case of the ambient-pressure sample, two-dimensional CuO_2 planes are not involved in the structure, as deduced from the above-proposed models.

CONCLUSIONS

A new oxide with the $LaBaCuGaO_5$ composition and brownmillerite-related structure has been synthesized, in which CuO_6 layers alternate in an ordered way with GaO_4 layers along the *a* direction. The disorder observed can be attributed to the presence of some equatorial oxygen atoms that must be arranged in a disordered way in either of the *Ima*2 and/or *Pmna* space groups.

The application of high pressure induces a phase transition $A_2B_2O_5 \rightarrow A_3B_3O_8$ that is favored by the replacement of Ba by Sr, involving an oxidation process.

ACKNOWLEDGMENTS

Financial support through Research Project MAT 98-0648 is acknowledged. The authors are grateful to Professors M. Takano (Kyoto University) and O. Terasaki (Tohoku University) for helpful discussions and Dr. J. Velázquez for his helpful advice.

REFERENCES

1. M. Isobe, Y. Matsui, and E. Takayama-Muromachi, *Phys. C* **222,** 310 (1994).
2. E. Takayama-Muromachi and M. Isobe, *Jpn. J. Appl. Phys.* **33,** L1399 (1994).
3. J. Ramírez-Castellanos, Y. Matsui, M. Isobe, and E. Takayama-Muromachi, *J. Solid State Chem.* **123,** 378 (1996).

4. E. F. Bertaut, P. Blum, and A. Sagnières, *Acta Crystallogr.* **12,** 149 (1959).
5. J. T. Vaughey, J. B. Wiley, and K. R. Poeppelmeier, *Z. Anorg. Allg. Chem.* **598–599,** 327 (1991).
6. G. Roth, P. Adelmann, R. Knitte, S. Massing, and T. H.Wolf, *J. Solid State Chem.* **99,** 376 (1992).
7. A. L. Kharlanov, E. V. Antipov, I. Bryntse, A. V. Luzikova, and L. M. Kovba, *Eur. J. Solid State Inorg. Chem.* **29,** 1041 (1992).
8. A. V. Luzikova, A. L. Kharlanov, and E. V. Antipov, *Z. Anorg. Allg. Chem.* **620,** 326 (1994).
9. M. Takano, Y. Takeda, and O. Ohtaka, *in* "Encyclopedia of Inorganic Chemistry" (R. Bruce King, Ed.), Vol. 3, p. 1372, 1994.
10. R. Killas, MacTempas Software 1.7.2, Berkeley Laboratory (UCLA), Berkely, CA.
11. A. A. Colville and S. Geller, *Acta Crystallogr. B* **27,** 2311 (1971).
12. J. M. González-Calbet and J. Rodríguez, *Inst. Phys. Conf. Ser.* **93**(2), 379 (1988).
13. J. C. Grenier, J. Darriet, M. Pouchard, and P. Hagenmuller, *Mater. Res. Bull.* **11,** 1219 (1976).
14. R. D. Shannon, *Acta Crystallogr. A* **32,** 751 (1975).
15. M. A. Alario-Franco, M. J. R. Henche, M. Vallet, J. M. González, J. C. Grenier, A. Wattiaux, and P. Hagenmuller, *J. Solid State Chem.* **46,** 23 (1983).
16. J. Rodriguez, Ph.D. thesis, University of Barcelona, Spain, 1984.